

Anomalous spin Hall magnetoresistance in Pt/Co bilayers

Masashi Kawaguchi¹, Daiki Towa¹, Yong-Chang Lau^{1,2}, Saburo Takahashi³ and Masamitsu Hayashi^{1,2*}

¹*Department of Physics, The University of Tokyo, Bunkyo, Tokyo 113-0033, Japan*

²*National Institute for Materials Science, Tsukuba 305-0047, Japan*

³*Institute for Materials Research, Tohoku University, Sendai 980-8577, Japan*

We have studied the spin Hall magnetoresistance (SMR), the magnetoresistance within the plane transverse to the current flow, of Pt/Co bilayers. We find that the SMR increases with increasing Co thickness: the effective spin Hall angle for bilayers with thick Co exceeds the reported values of Pt when a conventional drift-diffusion model is used. An extended model including spin transport within the Co layer cannot account for the large SMR. To identify its origin, contributions from other sources are studied. For most bilayers, the SMR increases with decreasing temperature and increasing magnetic field, indicating that magnon-related effects in the Co layer play little role. Without the Pt layer, we do not observe the large SMR found for the Pt/Co bilayers with thick Co. Implementing the effect of the so-called interface magnetoresistance and the textured induced anisotropic scattering cannot account for the Co thickness dependent SMR. Since the large SMR is present for W/Co but its magnitude reduces in W/CoFeB, we infer its origin is associated with a particular property of Co.

*Email: hayashi@phys.s.u-tokyo.ac.jp

The spin Hall effect¹⁻³ of heavy metals allows generation of spin current large enough to control the magnetization direction of a neighboring magnetic layer. The amount of spin current generated via the spin Hall effect is determined by the spin Hall angle and can vary depending on the strength of the spin orbit interaction, band filling and Berry curvature of particular orbitals, and the number of impurities that can cause spin dependent scattering. Significant effort has been made to study the spin Hall effect in heavy metal (HM)/ferromagnetic metal (FM) bilayer system as the spin current generated within the HM layer can induce magnetization switching and coherent precession, domain nucleation and domain wall motion in the FM layer.

The spin current generated by the spin Hall effect can in turn influence the charge current⁴. In particular, the resistance of bilayers consisting of a HM layer and a ferromagnetic insulator (FI) or FM layer changes depending on the magnetization direction of the FI or FM layer⁵⁻⁸. The effect, known as the spin Hall magnetoresistance (SMR), scales with the square of the spin Hall angle of the HM layer. Importantly, the way the resistance depends on the magnetization direction is distinct from that of the anisotropic magnetoresistance (AMR) that takes place in the FM layer. These features allow one to use the SMR as a convenient means to extract the magnitude of spin Hall angle of the HM layer: the spin Hall angle obtained through SMR seem to agree with that estimated by other methods⁹. Recently, studies on SMR related effects have been increasing¹⁰; an unidirectional component of the SMR is found in HM/FM bilayers¹¹, SMR has been observed in systems with antiferromagnets¹²⁻¹⁵, the observation of the spin Nernst effect is based on the SMR theory¹⁶⁻¹⁸ and the SMR analogue of the Rashba-Edelstein effect^{19,20} has been found in Bi based structures²¹.

The magnetoresistance (MR) of heterostructures that include Pt/Co bilayer has been under focus recently. A MR that scales with the inverse of the Co layer thickness has been reported in

Pt/Co/Pt trilayers²²⁻²⁴. Such interfacial contribution to the MR was found to be anisotropic: the MR is different when the (in-plane) magnetization points along or when it is orthogonal to the current flow. Similarly proximity induced magnetic moments of the Pt layer can contribute to the MR via AMR²⁵. Although not specific to the Pt/Co systems, it has been reported that texture induced anisotropic scattering can influence the MR²⁶⁻²⁸.

Here we report on a systematic study of the MR in Pt/Co bilayers. We show that an anomalously large SMR emerges in Pt/Co bilayers: the SMR increases with increasing Co thickness and the extracted effective spin Hall angle for such structures exceeds the expected value of Pt. An extended drift diffusion model that includes spin current generation and diffusion in the Co layer cannot account for the anomalous SMR. The SMR increases with decreasing temperature and increasing magnetic field for thick Co bilayers, suggesting that magnon-related effects in the Co layer has little influence on the enhancement of the SMR. The large SMR diminishes for films without the Pt layer; it is also found for W/Co but the effect is reduced for W/CoFeB. We thus infer that there is a process in Co that causes the SMR to increase with increasing Co thickness.

Samples are grown on silicon substrates coated with 100 nm thick oxide using RF magnetron sputtering. The film structure is sub.|0.5 Ta| d_N Pt| t_F Co|2 MgO|1 Ta (units of the thickness is nm). d_N and t_F represent the thickness of the HM and FM layers, respectively. A 0.5 nm thick Ta layer is used as a seed layer for the growth of the Pt layer. The MgO|Ta is used as a capping layer. Hall bars are created via shadow masking the deposition. The width of the Hall bars is ~ 0.4 mm and the distance between the voltage probes to measure the resistance is $\sim 1.2-1.5$ mm. Transport measurements are carried out in He-filled cryostat (Quantum Design, Physical Properties Measurement System).

The inset of Fig. 1(a) shows a schematic of the film structure together with the definition of the coordinate system. Current is passed along the x -direction. The Pt and Co thickness dependence of the resistivity is plotted in Figs. 1(a) and 1(b), respectively. The resistivity is obtained by measuring the layer thickness dependence of the sheet conductance (G_{XX}). The fluctuation in the resistivity for thin Pt and/or Co layer films arises since the resistivity is estimated from the thickness derivative of the sheet conductance. (See the Supplementary Material (Fig. S1) for the details of the extraction of the resistivity.) The resistivity of the Pt and Co layers shows a significant thickness dependence most likely due to increased interface scattering when the thickness is reduced^{6,23,29}.

The MR of the Pt/Co bilayers are shown in Fig. 2. We measure the resistance (R_{XX}) of the Hall bars while rotating the magnetic field in the y - z plane. We define the angle between the magnetic field (H) and the z -axis within the y - z plane as φ (see Fig. 1(a)). The φ dependence of R_{XX} is fitted with a sinusoidal function $R_{XX} = R_0 \left[1 - \frac{\Delta R_{y-z}}{2} \cos(2\varphi + \varphi_0) \right]$. From hereafter, we refer to ΔR_{y-z} as the SMR even though it may contain contributions from other MR effects. ΔR_{y-z} is plotted as a function of the Pt thickness (d_{Pt}) and Co thickness (t_{Co}) in Figs. 2(a-e) and 2(f-i), respectively. The phase offset φ_0 is nearly zero for all films. R_0 is used to estimate the sheet conductance G_{XX} .

For a given Co thickness, the characteristics of the Pt thickness dependence of ΔR_{y-z} is similar to what has been reported previously in similar systems⁵⁻⁸: $|\Delta R_{y-z}|$ takes a maximum and gradually decreases with increasing d_{Pt} . The trend is in agreement with the drift diffusion model established to describe the spin Hall magnetoresistance^{4,8} and can be considered as a fingerprint of SMR. In contrast, the Co thickness dependence of ΔR_{y-z} is different from what the drift

diffusion model predicts. ΔR_{y-z} increases with increasing t_{Co} and the Co thickness at which $|\Delta R_{y-z}|$ saturates depends on d_{Pt} . According to the model, however, $|\Delta R_{y-z}|$ should roughly scale with $1/t_{Co}$ due to current shunting into the Co layer.

To illustrate the unusual characteristics of the ΔR_{y-z} found in the Pt/Co bilayers, we fit the Pt thickness dependence of the normalized ΔR_{y-z} with the drift-diffusion model. ΔR_{y-z} is normalized by a factor (x_N) that takes into account current shunting into the Co layer: $x_N = (d_N \rho_F) / (d_N \rho_F + t_F \rho_N)$, where ρ_N (ρ_F) and d_N (t_F) represent the resistivity and thickness of the HM (FM) layers, respectively. (Note that $N=Pt$ and $F=Co$ in the experiments.) $\Delta R_{y-z}/x_N$ is plotted as a function of d_N in Fig. 3(a). In the drift-diffusion model, here we assume transparent HM/FM interface and zero longitudinal spin absorption into the FM layer⁸, which returns the lower limit of the effective spin Hall angle θ_{SH} . The equation used for the fitting is:

$$\frac{\Delta R_{y-z}}{x_N} = -\theta_{SH}^2 \frac{\lambda_N}{d_N} \tanh\left(\frac{d_N}{2\lambda_N}\right) \left[1 - \frac{1}{\cosh(d_N/\lambda_N)}\right] \quad (1)$$

where λ_N is the spin diffusion length of the HM layer. λ_N and θ_{SH} are the fitting parameters and the resulting fitted curves are shown in Fig. 3(a). The agreement between the experimental results and Eq. (1) are quite good.

In Fig. 3(b) and 3(c), we show the Co thickness dependence of λ_N and θ_{SH} obtained from the fitting. We find that λ_N shows little dependence on t_{Co} whereas θ_{SH} increases with increasing t_{Co} . The estimated θ_{SH} does not seem to saturate with Co thickness of ~ 7 nm and the maximum value obtained at $t_{Co} \sim 7$ nm exceeds the effective spin Hall angle of Pt reported thus far³⁰⁻³². We have also studied the FM layer thickness dependence of HM/FM bilayers with HM=W and found again an extraordinary large SMR ($\Delta R_{y-z}/x_N$) only when the FM layer is Co (see Supplementary

material Fig. S2): $\Delta R_{y-z}/x_N$ matches the value of the drift-diffusion model for FM=CoFeB, as reported previously^{8,9,33}. We thus consider the large $\Delta R_{y-z}/x_N$ found in Pt/Co bilayers is likely due to bulk spin transport in the Co layer.

Since the SMR increases with increasing Co thickness, one may consider spin current generation within the Co layer via excitations of magnons. Magnon is the main carrier of spin current in ferromagnetic insulators (FI) and causes the spin Seebeck effect in HM/FI structures³⁴. Any magnon related effect, however, will be suppressed by application of large magnetic field or by lowering the measurement temperature³⁵. We have thus studied the field and temperature dependence of the SMR of Pt/Co bilayers for selected films.

Figure 4(a) shows ΔR_{y-z} plotted as a function of the magnitude of the magnetic field $|H|$. Here we have measured the bilayer resistance against the magnetic field directed along the y - (R_{xx}^y) and z - (R_{xx}^z) axes and took their difference, i.e., $\Delta R_{y-z}=(R_{xx}^y-R_{xx}^z)/R_{xx}^z$. The definition of ΔR_{y-z} is similar to that described above using the sinusoidal function if one assumes $R_{xx}^z \sim R_0$. In all cases, we find $|\Delta R_{y-z}|$ slightly increases with increasing $|H|$. (For $|H|$ smaller than ~ 15 kOe, the hard axis magnetic field is not sufficient to force the magnetization to point along the field direction, thus ΔR_{y-z} decreases with decreasing $|H|$.) We consider the slight increase in $|\Delta R_{y-z}|$ with increasing $|H|$ above ~ 15 kOe may originate from contribution of the so-called Hanle magnetoresistance^{36,37}, which causes an increase in R_{xx}^z with increasing $|H|$ and thus results in enhancement of $|\Delta R_{y-z}|$. Although the Hanle magnetoresistance may influence $|\Delta R_{y-z}|$, we do not find significant reduction of $|\Delta R_{y-z}|$ at large $|H|$ similar to that reported for the magnetic field dependence of the spin Seebeck coefficient in Pt/YIG³⁵.

The temperature dependence of ΔR_{y-z} is plotted in Fig. 4(b). Except for Pt/Co bilayer with $d_N \sim 8$ nm and $t_F \sim 1$ nm, $|\Delta R_{y-z}|$ increases with decreasing temperature. The change is more pronounced for films with larger t_F and/or d_N . The temperature dependence of ΔR_{y-z} is similar to what has been found in metallic bilayers: $|\Delta R_{y-z}|$ increases with decreasing temperature which has been attributed to the change in the degree of spin absorption⁸. Since we do not find any reduction in $|\Delta R_{y-z}|$ at low temperature, we consider any magnon-related effect is almost negligible for the anomalously large SMR for thicker Co bilayers.

As $|\Delta R_{y-z}|$ becomes larger when the Co thickness is increased, we infer the enhancement is due to an effect that takes place in the bulk of the Co layer. Since the spin diffusion length of Co is reported to be much larger than the film thickness used here³⁸, it may be feasible to consider spin current generation within the Co layer via, e.g. anomalous Hall and/or spin Hall effects. One can include contributions from the anomalous Hall and spin Hall effects of the FM layer (as well as longitudinal and transverse spin-current absorption) into the drift-diffusion model and estimate the resulting SMR (R_{SMR}).

$$R_{\text{SMR}} = -(1 - x_N)x_N\theta_{AH}^2 - (1 - x_N)(1 - P^2)\theta_F^2 \frac{2\lambda_F}{t_F} \tanh\left(\frac{t_F}{2\lambda_F}\right) - x_N\theta_{SH}^2 \frac{\lambda_N}{d_N} \tanh^2\left(\frac{d_N}{2\lambda_N}\right) \left\{ \text{Re} \left[\frac{g_S}{1 + g_S \coth(d_N/\lambda_N)} \right] - \frac{(1 + \zeta)^2 g_F}{1 + g_F \coth(d_N/\lambda_N)} \right\} \quad (2)$$

where $g_S = \rho_N \lambda_N G_{\text{MIX}}$, $g_F = (1 - P^2) \frac{\rho_N \lambda_N}{\rho_F \lambda_F} \tanh\left(\frac{t_F}{\lambda_F}\right)$, $\zeta = \frac{\theta_F \lambda_F \tanh(t_F/2\lambda_F)}{\theta_{SH} \lambda_N \tanh(d_N/2\lambda_N)}$. G_{MIX} is the spin mixing conductance of the HM/FM interface, θ_F , θ_{AH} , λ_F and P are the spin Hall angle, anomalous Hall angle, spin diffusion length and spin polarization of the FM layer. The first and second terms of the right-hand side of Eq. (2) represent contributions to ΔR_{y-z} from the

anomalous Hall and spin Hall effects of the FM layer, respectively. The second term in the curly bracket represents the longitudinal spin absorption contribution to the SMR⁸. This term is modified ($\zeta \neq 0$) when the FM spin Hall effect is considered. With $\theta_F = \theta_{AH} = 0$, $\text{Re}[G_{\text{MIX}}] \gg \text{Im}[G_{\text{MIX}}]$ and $\text{Re}[G_{\text{MIX}}] \gg 1/(2\rho_N\lambda_N)$, we recover Eq. (1). The transverse spin diffusion length^{39,40} of the FM layer is assumed to be zero here.

Representative values of the calculated R_{SMR} are shown in the supplementary material (Fig. S4). In the calculations, the spin Hall angle of Pt is set to one of the largest values reported thus far ($\theta_{SH} \sim 0.2$)³⁰, the anomalous Hall angle is obtained from the measurements (the largest value of the Pt/Co bilayers is ~ 0.03 , see Fig. S3) and the spin Hall angle of Co is estimated using the relationship $\theta_{AH} \sim P\theta_F$: here we use $P \sim 0.4$. Although the magnitude of R_{SMR} can be adjusted to match the experimental results of ΔR_{y-z} , it is difficult to reproduce the characteristics found in the experiments shown in Fig. 2, the increasing ΔR_{y-z} with increasing Co thickness.

We have also studied the MR within the x - z plane which provides information on the so-called anisotropic interface magnetoresistance²²⁻²⁴ (for clarity of notation, we denote such MR as IMR instead of AIMR used in Ref. ²²). R_{XX} is measured while the magnetic field is rotated in the x - z plane. The angle between the magnetic field and the z -axis within the x - z plane is defined as γ . We fit the γ dependence of R_{XX} using a sinusoidal function $R_{XX} = R_0 \left[1 - \frac{\Delta R_{x-z}}{2} \cos(2\gamma + \gamma_0) \right]$. ΔR_{x-z} is plotted as a function of Co thickness (t_{Co}) in Fig. 5(a). The large t_{Co} limit of ΔR_{x-z} normalized by the current flowing in the Co layer, i.e. $\frac{\Delta R_{x-z}}{1-x_N}$, gives the anisotropic magnetoresistance (AMR) of bulk Co (R_{AMR}) whereas changes at smaller t_{Co} reflect contribution from the interface(s). In Fig. 5(b), we plot $\frac{\Delta R_{x-z}}{1-x_N}$ vs. $1/t_{\text{Co}}$. The y -axis intercept of the linear

fitting in the appropriate t_{Co} range, as shown in Fig. 5(b), gives R_{AMR} . We find that R_{AMR} for films with different Pt thickness are nearly the same ($R_{\text{AMR}} \sim 1.6\%$), which is close to what has been reported previously⁴¹. IMR is obtained by the following relation, $R_{\text{IMR}} \equiv \frac{\Delta R_{x-z}}{1-x_N} - R_{\text{AMR}}$. The Pt thickness dependence of R_{IMR} is plotted in Fig. 5(c). As reported previously^{21,23,24}, R_{IMR} increases with decreasing t_{Co} .

Although the microscopic mechanism is not clear, one may assume^{23,24} that R_{IMR} is isotropic within the film plane, i.e. R_{IMR} contributes to the y - z plane MR in the same way it does in the x - z plane. Assuming a parallel circuit that includes contribution from the SMR within the HM layer (R_{SMR}) and the IMR that takes place in the FM layer (R_{IMR}), we obtain an expression for ΔR_{y-z} , which can be rewritten as: $R_{\text{SMR}} = \Delta R_{y-z} \frac{1}{x_N} - (R_{\text{IMR}} + \Delta R_{y-z}^{\text{Co}}) \frac{t_F \rho_N}{\rho_F d_N}$ (see Supplementary material for the derivation). Here we have also subtracted ΔR_{y-z} for films with $d_{\text{Pt}}=0$, which is denoted as $\Delta R_{y-z}^{\text{Co}}$. $\Delta R_{y-z}^{\text{Co}}$ is not related to SMR and is likely associated with the textured induced anisotropic scattering (also referred to as the geometrical size effect²⁷). In Fig. 5(d), R_{SMR} is plotted as a function of d_{Pt} . As evident, $|R_{\text{SMR}}|$ increases with increasing Co thickness, which cannot be described by the extended drift diffusion model (including spin transport within the FM layer), i.e. Eq. (2). Moreover, the sign of R_{SMR} reverses when $d_{\text{Pt}} \sim 2$ -3 nm and its magnitude increases with decreasing d_{Pt} : see the inset of Fig. 5(d). Such trend of R_{SMR} , inconsistent with the d_{Pt} dependence of SMR, is largely caused by the subtraction of the R_{IMR} term. These results show that the large ΔR_{y-z} which increases with the Co thickness cannot be described by combinations of SMR, an isotropic IMR and texture induced anisotropic scattering.

Since ΔR_{y-z} increases with t_{Co} , interface effects (e.g. spin memory loss⁴², proximity magnetization induced AMR²⁵, spin orbit interface AMR^{43,44}, Edelstein magnetoresistance^{20,21},

enhanced spin Hall effect at the interface⁴⁵) may not play a dominant role in setting the SMR found here. It is also difficult to foresee thermal effects (e.g. anomalous Nernst effect⁴⁶) give rise to the large SMR since we find nearly symmetric resistance levels for positive and negative magnetic field in all field directions¹⁷. It has been suggested that the magnetoresistance due to texture induced anisotropic scattering in the FM layer can be enhanced by attaching a NM layer with large spin orbit interaction (the length scale of such MR is associated with the electron mean free path of the FM layer)²⁸. With respect to the texture of the Co layer, we find a large ΔR_{y-z} both in Pt/Co and W/Co bilayers despite the different texture of the HM underlayer. Furthermore, ΔR_{y-z} of Ta/Co bilayers (i.e. the case when $d_{Pt}=0$) shows a much reduced ΔR_{y-z} compared to that of W/Co bilayers. Since Ta and W are both amorphous-like⁹, the texture of the Co layer is expected to be similar for the two bilayers. We thus infer that the texture of the Co film has little to do with the large ΔR_{y-z} . It is possible that the spin orbit coupling at the interface may be different for the three HM layers (Pt, W and Ta), as manifested by the difference in the Dzyaloshinskii-Moriya interaction^{47,48}, and may influence the MR by means of anisotropic scattering. As the microscopic origin of the such effect remains to be identified, further investigation is required to clarify its presence.

In summary, we have studied the Pt and Co thickness dependence of spin Hall magnetoresistance), the magnetoresistance within the plane transverse to the current flow, in Pt/Co bilayers. We find SMR that increases with increasing Co thickness, which cannot be fully accounted for even if the anomalous Hall and spin Hall effects of the Co layer are considered. Other effects that may contribute to the MR are evaluated to assess their influence on the SMR. We find that the so-called anisotropic interface magnetoresistance and the magnetoresistance due

to texture induced anisotropic scattering cannot describe the large SMR observed here. Further investigation is required to clarify the origin of the SMR in HM/Co bilayers.

Supplementary Material

The following topics are included in the supplementary material: description on how the thickness dependent resistivity is obtained, additional experimental results on the anomalous Hall resistance of Pt/Co bilayers and SMR of W/Co and W/CoFeB bilayers, model calculations of the SMR using the drift-diffusion model, and description of how IMR is extracted.

Acknowledgements

We thank S. Mitani for fruitful discussion. This work was partly supported by JSPS Grant-in-Aids for Specially Promoted Research (15H05702), Casio Foundation, and the Center of Spintronics Research Network of Japan. Y.-C.L. is a JSPS international research fellow.

References

- 1 M. I. D'yakonov and V. I. Perel', "Possibility of Orienting Electron Spins with Current." *Jetp Letters-Ussr* **13**, 467 (1971).
- 2 Y. K. Kato, R. C. Myers, A. C. Gossard, and D. D. Awschalom, "Observation of the Spin Hall Effect in Semiconductors." *Science* **306**, 1910 (2004).
- 3 L. Liu, C.-F. Pai, Y. Li, H. W. Tseng, D. C. Ralph, and R. A. Buhrman, "Spin-Torque Switching with the Giant Spin Hall Effect of Tantalum." *Science* **336**, 555 (2012).
- 4 Y. T. Chen, S. Takahashi, H. Nakayama, M. Althammer, S. T. B. Goennenwein, E. Saitoh, and G. E. W. Bauer, "Theory of Spin Hall Magnetoresistance." *Phys. Rev. B* **87** 144411 (2013).
- 5 H. Nakayama, M. Althammer, Y. T. Chen, K. Uchida, Y. Kajiwara, D. Kikuchi, T. Ohtani, S. Geprags, M. Opel, S. Takahashi, R. Gross, G. E. W. Bauer, S. T. B. Goennenwein, and E. Saitoh, "Spin Hall Magnetoresistance Induced by a Nonequilibrium Proximity Effect." *Phys. Rev. Lett.* **110** 206601 (2013).
- 6 M. Althammer, S. Meyer, H. Nakayama, M. Schreier, S. Altmannshofer, M. Weiler, H. Huebl, S. Gepraegs, M. Opel, R. Gross, D. Meier, C. Klewe, T. Kuschel, J.-M. Schmalhorst, G. Reiss, L. Shen, A. Gupta, Y.-T. Chen, G. E. W. Bauer, E. Saitoh, and S. T. B. Goennenwein, "Quantitative Study of the Spin Hall Magnetoresistance in Ferromagnetic Insulator/Normal Metal Hybrids." *Phys. Rev. B* **87** 224401 (2013).
- 7 C. Hahn, G. de Loubens, O. Klein, M. Viret, V. V. Naletov, and J. Ben Youssef, "Comparative Measurements of Inverse Spin Hall Effects and Magnetoresistance in Yig/Pt and Yig/Ta." *Phys. Rev. B* **87** 174417 (2013).
- 8 J. Kim, P. Sheng, S. Takahashi, S. Mitani, and M. Hayashi, "Spin Hall Magnetoresistance in Metallic Bilayers." *Phys. Rev. Lett.* **116** 097201 (2016).
- 9 J. Liu, T. Ohkubo, S. Mitani, K. Hono, and M. Hayashi, "Correlation between the Spin Hall Angle and the Structural Phases of Early 5d Transition Metals." *Appl. Phys. Lett.* **107** 232408 (2015).
- 10 Y. T. Chen, S. Takahashi, H. Nakayama, M. Althammer, S. T. B. Goennenwein, E. Saitoh, and G. E. W. Bauer, "Theory of Spin Hall Magnetoresistance (Smr) and Related Phenomena." *J. Phys.-Condes. Matter* **28**, 15 103004 (2016).
- 11 C. O. Avci, K. Garello, A. Ghosh, M. Gabureac, S. F. Alvarado, and P. Gambardella, "Unidirectional Spin Hall Magnetoresistance in Ferromagnet/Normal Metal Bilayers." *Nat. Phys.* **11**, 570 (2015).
- 12 A. Manchon, "Spin Hall Magnetoresistance in Antiferromagnet/Normal Metal Bilayers." *Physica Status Solidi-Rapid Research Letters* **11**, 5 1600409 (2017).
- 13 Y. Ji, J. Miao, K. K. Meng, Z. Y. Ren, B. W. Dong, X. G. Xu, Y. Wu, and Y. Jiang, "Spin Hall Magnetoresistance in an Antiferromagnetic Magnetoelectric Cr₂O₃/Heavy-Metal W Heterostructure." *Appl. Phys. Lett.* **110**, 4 262401 (2017).
- 14 J. Fischer, O. Gomonay, R. Schlitz, K. Ganzhorn, N. Vlietstra, M. Althammer, H. Huebl, M. Opel, R. Gross, S. T. B. Goennenwein, and S. Geprägs, "Spin Hall Magnetoresistance in Antiferromagnet/Normal Metal Heterostructures." arXiv:1709.04158.
- 15 T. Shang, Q. F. Zhan, H. L. Yang, Z. H. Zuo, Y. L. Xie, L. P. Liu, S. L. Zhang, Y. Zhang, H. H. Li, B. M. Wang, Y. H. Wu, S. Zhang, and R. W. Li, "Effect of Nio Inserted Layer on Spin-Hall Magnetoresistance in Pt/Nio/Yig Heterostructures." *Appl. Phys. Lett.* **109**, 4 032410 (2016).

- 16 S. Meyer, Y. T. Chen, S. Wimmer, M. Althammer, T. Wimmer, R. Schlitz, S. Gepraegs, H. Huebl, D. Koedderitzsch, H. Ebert, G. E. W. Bauer, R. Gross, and S. T. B. Goennenwein, "Observation of the Spin Nernst Effect." *Nat. Mater.* **16**, 977 (2017).
- 17 P. Sheng, Y. Sakuraba, Y.-C. Lau, S. Takahashi, S. Mitani, and M. Hayashi, "The Spin Nernst Effect in Tungsten." *Science Advances* **3**, e1701503 (2017).
- 18 D.-J. Kim, C.-Y. Jeon, J.-G. Choi, J. W. Lee, S. Surabhi, J.-R. Jeong, K.-J. Lee, and B.-G. Park, "Observation of Transverse Spin Nernst Magnetoresistance Induced by Thermal Spin Current in Ferromagnet/Non-Magnet Bilayers." *Nat. Commun.* **8**, 1400 (2017).
- 19 I. M. Miron, K. Garello, G. Gaudin, P. J. Zermatten, M. V. Costache, S. Auffret, S. Bandiera, B. Rodmacq, A. Schuhl, and P. Gambardella, "Perpendicular Switching of a Single Ferromagnetic Layer Induced by in-Plane Current Injection." *Nature* **476**, 189 (2011).
- 20 J. C. Rojas Sanchez, L. Vila, G. Desfonds, S. Gambarelli, J. P. Attane, J. M. De Teresa, C. Magen, and A. Fert, "Spin-to-Charge Conversion Using Rashba Coupling at the Interface between Non-Magnetic Materials." *Nat. Commun.* **4**, 7 2944 (2013).
- 21 H. Nakayama, Y. Kanno, H. Y. An, T. Tashiro, S. Haku, A. Nomura, and K. Ando, "Rashba-Edelstein Magnetoresistance in Metallic Heterostructures." *Phys. Rev. Lett.* **117**, 6 116602 (2016).
- 22 A. Kobs, S. Hesse, W. Kreuzpaintner, G. Winkler, D. Lott, P. Weinberger, A. Schreyer, and H. P. Oepen, "Anisotropic Interface Magnetoresistance in Pt/Co/Pt Sandwiches." *Phys. Rev. Lett.* **106** 217207 (2011).
- 23 A. Kobs and H. P. Oepen, "Disentangling Interface and Bulk Contributions to the Anisotropic Magnetoresistance in Pt/Co/Pt Sandwiches." *Phys. Rev. B* **93**, 6 014426 (2016).
- 24 X. Xiao, J. X. Li, Z. Ding, J. H. Liang, L. Sun, and Y. Z. Wu, "Unusual Angular Dependent Magnetoresistance in Single-Crystalline Co/Pt Bilayers." *Appl. Phys. Lett.* **108**, 4 222402 (2016).
- 25 S. Y. Huang, X. Fan, D. Qu, Y. P. Chen, W. G. Wang, J. Wu, T. Y. Chen, J. Q. Xiao, and C. L. Chien, "Transport Magnetic Proximity Effects in Platinum." *Phys. Rev. Lett.* **109** 107204 (2012).
- 26 T. G. S. M. Rijks, S. K. J. Lenczowski, R. Coehoorn, and W. J. M. deJonge, "In-Plane and out-of-Plane Anisotropic Magnetoresistance in Ni₈₀Fe₂₀ Thin Films." *Phys. Rev. B* **56**, 362 (1997).
- 27 W. Gil, D. Gorlitz, M. Horisberger, and J. Kotzler, "Magnetoresistance Anisotropy of Polycrystalline Cobalt Films: Geometrical-Size and Domain Effects." *Phys. Rev. B* **72**, 10 134401 (2005).
- 28 L. K. Zou, Y. Zhang, L. Gu, J. W. Cai, and L. Sun, "Tunable Angular-Dependent Magnetoresistance Correlations in Magnetic Films and Their Implications for Spin Hall Magnetoresistance Analysis." *Phys. Rev. B* **93** 075309 (2016).
- 29 G. Fischer, H. Hoffmann, and J. Vancea, "Mean Free Path and Density of Conductance Electrons in Platinum Determined by the Size Effect in Extremely Thin Films." *Phys. Rev. B* **22**, 6065 (1980).
- 30 W. Zhang, W. Han, X. Jiang, S.-H. Yang, and S. S. P. Parkin, "Role of Transparency of Platinum-Ferromagnet Interfaces in Determining the Intrinsic Magnitude of the Spin Hall Effect." *Nat. Phys.* **11**, 496 (2015).
- 31 C.-F. Pai, Y. Ou, L. H. Vilela-Leao, D. C. Ralph, and R. A. Buhrman, "Dependence of the Efficiency of Spin Hall Torque on the Transparency of Pt/Ferromagnetic Layer Interfaces." *Phys. Rev. B* **92** 064426 (2015).

- 32 M. H. Nguyen, D. C. Ralph, and R. A. Buhrman, "Spin Torque Study of the Spin Hall Conductivity and Spin Diffusion Length in Platinum Thin Films with Varying Resistivity." *Phys. Rev. Lett.* **116**, 6 126601 (2016).
- 33 J. G. Choi, J. W. Lee, and B. G. Park, "Spin Hall Magnetoresistance in Heavy-Metal/Metallic-Ferromagnet Multilayer Structures." *Phys. Rev. B* **96**, 8 174412 (2017).
- 34 K. Uchida, J. Xiao, H. Adachi, J. Ohe, S. Takahashi, J. Ieda, T. Ota, Y. Kajiwara, H. Umezawa, H. Kawai, G. E. W. Bauer, S. Maekawa, and E. Saitoh, "Spin Seebeck Insulator." *Nat. Mater.* **9**, 894 (2010).
- 35 T. Kikkawa, K. Uchida, S. Daimon, Z. Y. Qiu, Y. Shiomi, and E. Saitoh, "Critical Suppression of Spin Seebeck Effect by Magnetic Fields." *Phys. Rev. B* **92** 064413 (2015).
- 36 M. I. Dyakonov, "Magnetoresistance Due to Edge Spin Accumulation." *Phys. Rev. Lett.* **99** 126601 (2007).
- 37 S. Velez, V. N. Golovach, A. Bedoya-Pinto, M. Isasa, E. Sagasta, M. Abadia, C. Rogero, L. E. Hueso, F. S. Bergeret, and F. Casanova, "Hanle Magnetoresistance in Thin Metal Films with Strong Spin-Orbit Coupling." *Phys. Rev. Lett.* **116**, 6 016603 (2016).
- 38 J. Bass and W. P. Pratt, "Current-Perpendicular (Cp) Magnetoresistance in Magnetic Metallic Multilayers." *J. Magn. Magn. Mater.* **200**, 274 (1999).
- 39 T. Taniguchi, S. Yakata, H. Imamura, and Y. Ando, "Determination of Penetration Depth of Transverse Spin Current in Ferromagnetic Metals by Spin Pumping." *Appl. Phys. Express* **1** 031302 (2008).
- 40 A. Ghosh, S. Auffret, U. Ebels, and W. E. Bailey, "Penetration Depth of Transverse Spin Current in Ultrathin Ferromagnets." *Phys. Rev. Lett.* **109** 127202 (2012).
- 41 T. R. McGuire and R. I. Potter, "Anisotropic Magnetoresistance in Ferromagnetic 3d Alloys." *IEEE Trans. Magn.* **11**, 1018 (1975).
- 42 J. C. Rojas-Sanchez, N. Reyren, P. Laczkowski, W. Savero, J. P. Attane, C. Deranlot, M. Jamet, J. M. George, L. Vila, and H. Jaffres, "Spin Pumping and Inverse Spin Hall Effect in Platinum: The Essential Role of Spin-Memory Loss at Metallic Interfaces." *Phys. Rev. Lett.* **112** 106602 (2014).
- 43 V. L. Grigoryan, W. Guo, G. E. W. Bauer, and J. Xiao, "Intrinsic Magnetoresistance in Metal Films on Ferromagnetic Insulators." *Phys. Rev. B* **90** 161412 (2014).
- 44 S. S. L. Zhang and S. F. Zhang, "Angular Dependence of Anisotropic Magnetoresistance in Magnetic Systems." *J. Appl. Phys.* **115** 17c703 (2014).
- 45 L. Wang, R. J. H. Wesselink, Y. Liu, Z. Yuan, K. Xia, and P. J. Kelly, "Giant Room Temperature Interface Spin Hall and Inverse Spin Hall Effects." *Phys. Rev. Lett.* **116**, 6 196602 (2016).
- 46 C. O. Avci, K. Garello, M. Gabureac, A. Ghosh, A. Fuhrer, S. F. Alvarado, and P. Gambardella, "Interplay of Spin-Orbit Torque and Thermoelectric Effects in Ferromagnet/Normal-Metal Bilayers." *Phys. Rev. B* **90** 224427 (2014).
- 47 J. Torrejon, J. Kim, J. Sinha, S. Mitani, M. Hayashi, M. Yamanouchi, and H. Ohno, "Interface Control of the Magnetic Chirality in Cofeb/Mgo Heterostructures with Heavy-Metal Underlayers." *Nat. Commun.* **5** 4655 (2014).
- 48 I. Gross, L. J. Martínez, J. P. Tetienne, T. Hingant, J. F. Roch, K. Garcia, R. Soucaille, J. P. Adam, J. V. Kim, S. Rohart, A. Thiaville, J. Torrejon, M. Hayashi, and V. Jacques, "Direct Measurement of Interfacial Dzyaloshinskii-Moriya Interaction in X|Cofeb|Mgo Heterostructures with a Scanning Nv Magnetometer (X=Ta, Tan, and W)." *Phys. Rev. B* **94**, 064413 (2016).

Figure captions

Figure 1. (a) Pt layer thickness dependence of the resistivity of Pt (ρ_{Pt}) and (b) Co layer thickness dependence of the resistivity of Co (ρ_{Co}) in Pt/Co bilayer. Lines are guide to the eyes. The inset to (a) shows a schematic view of the system and definition of the coordinate axis.

Figure 2. (a) Magnetoresistance in the y - z plane (ΔR_{y-z}) plotted as a function of the Pt layer thickness (d_{Pt}) for fixed Co layer thicknesses. (f-j) ΔR_{y-z} vs. Co layer thickness (t_{Co}) for fixed Pt layer thicknesses. The thickness of the fixed thickness layer is noted in each panel.

Figure 3. (a) $\Delta R_{y-z}/x_N$ plotted as a function of Pt thickness. The thickness of the Co layer for each symbol is displayed in the legend. Solid lines show fitting results using Eq. (1). (b,c) Spin diffusion length λ_N (b) and the spin Hall angle θ_{SH} (c) of Pt obtained from the fitting shown in (a).

Figure 4. (a,b) Applied magnetic field (a) and the measurement temperature (b) dependence of ΔR_{y-z} for representative Pt/Co bilayers. The film structure is described in the legend.

Figure 5. (a) Magnetoresistance in the x - z plane (ΔR_{x-z}) plotted as a function of the Co layer thickness (t_{Co}) for fixed Pt layer thickness (d_{Pt}). (b) $\Delta R_{x-z}/(1 - x_N)$ vs. $1/t_{\text{Co}}$. The solid lines show linear fit to the data when $1/t_{\text{Co}}$ is small. The y -axis intercept of the linear line gives the AMR of bulk Co (R_{AMR}). (c) Interface magnetoresistance $R_{\text{IMR}} \equiv \frac{\Delta R_{x-z}}{1 - x_N} - R_{\text{AMR}}$ plotted as a

function of d_{Pt} . (d) $R_{SMR} = \Delta R_{y-z} \frac{1}{x_N} - (R_{IMR} + \Delta R_{y-z}^{Co}) \frac{t_F \rho_N}{\rho_F d_N}$ vs. d_{Pt} . The inset shows the same plot but with the vertical axis range expanded.

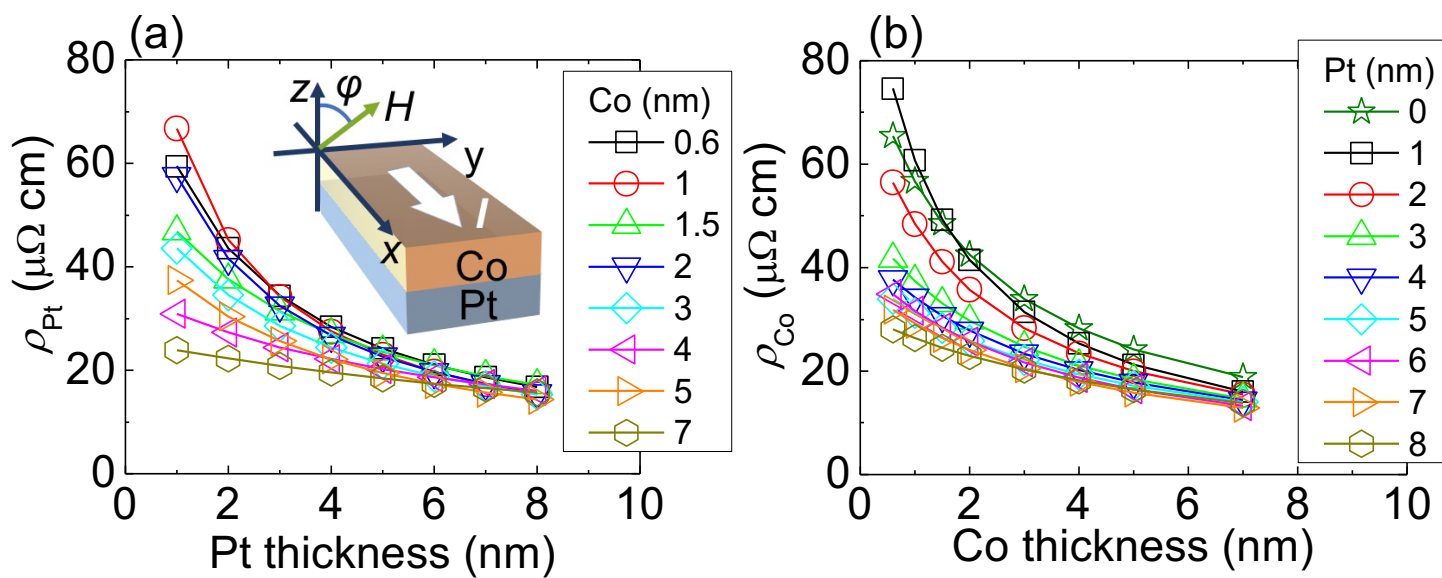


Fig. 1

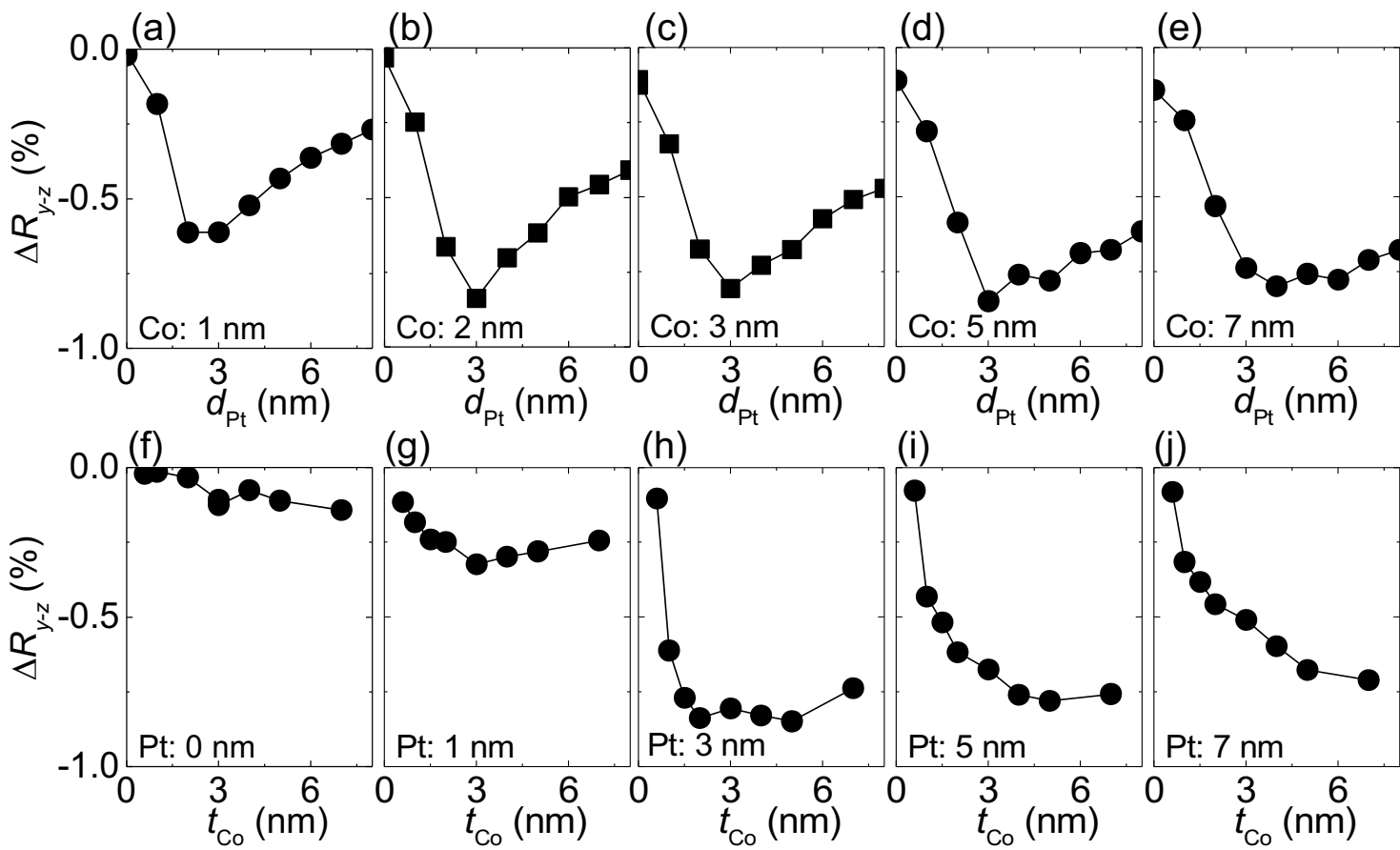


Fig. 2

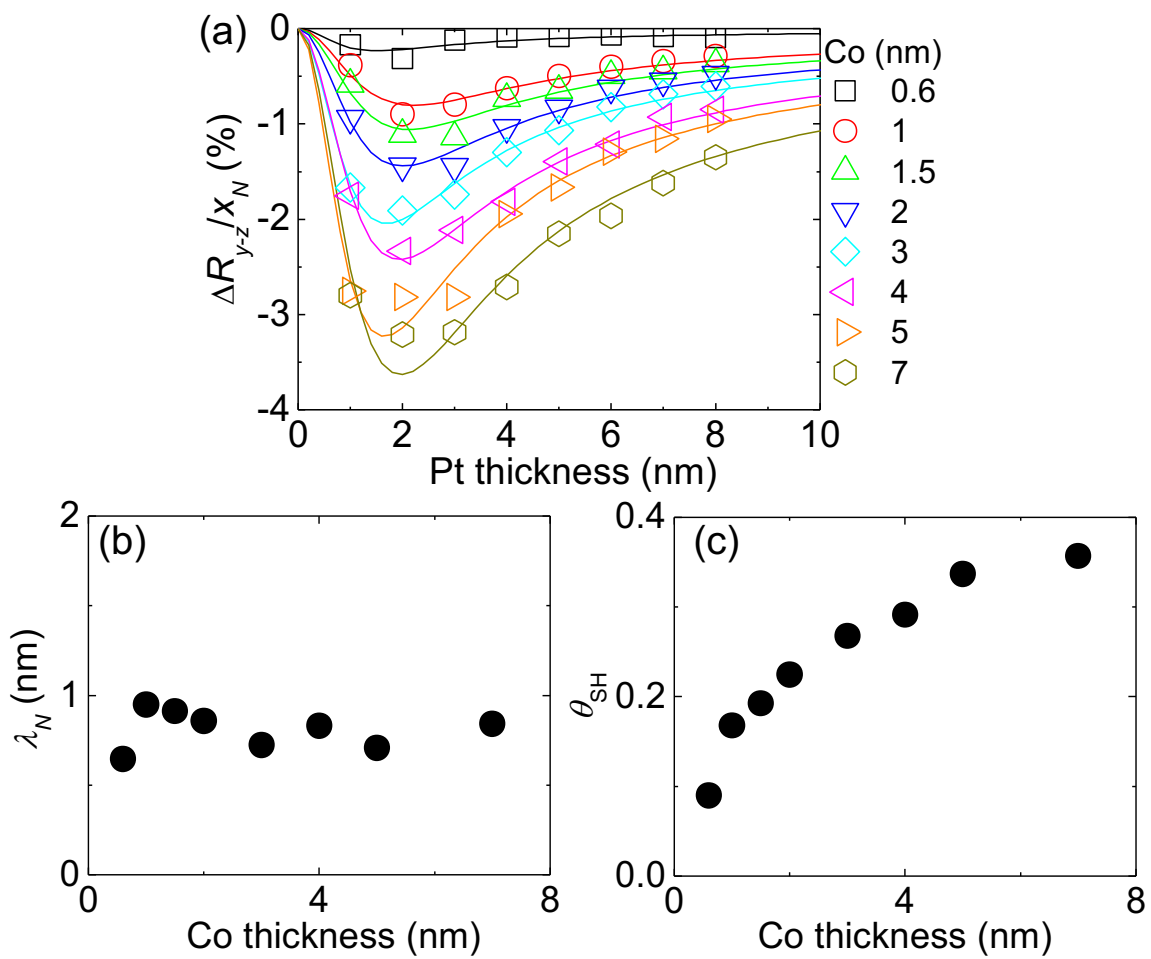


Fig. 3

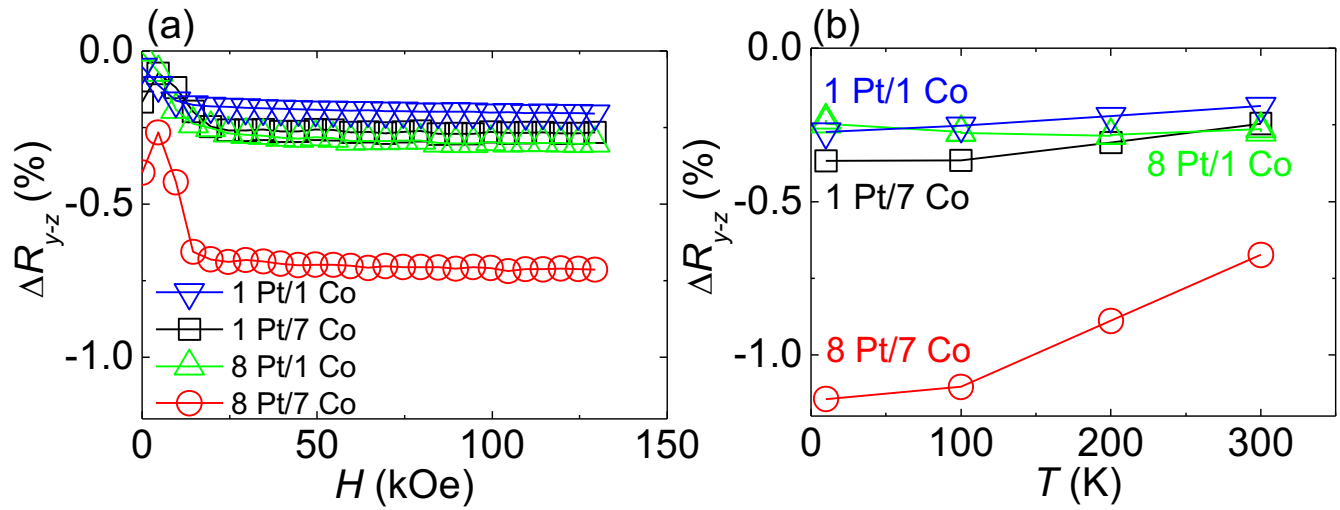


Fig. 4

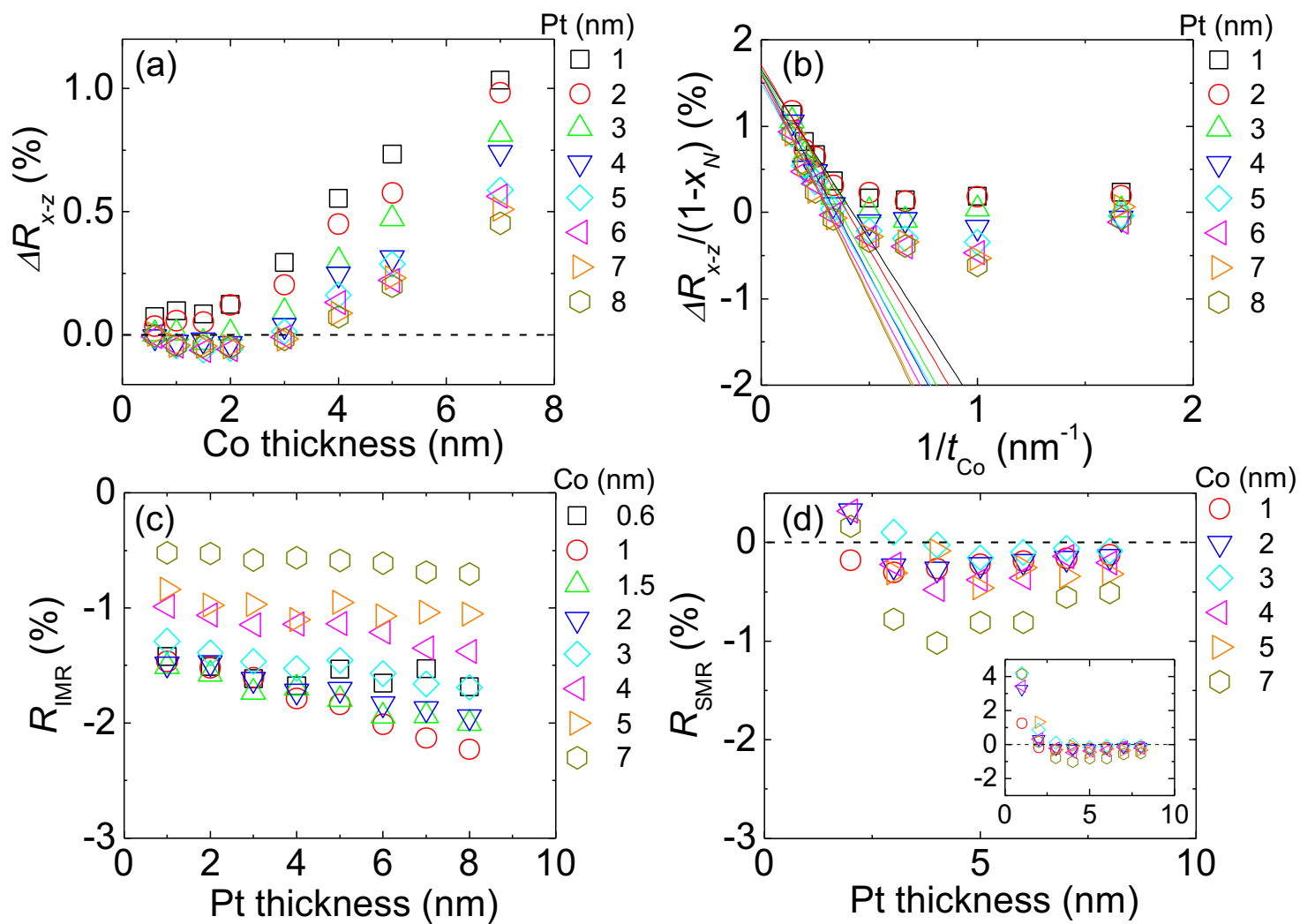


Fig. 5

Supplementary material for

Anomalous spin Hall magnetoresistance in Pt/Co bilayers

Masashi Kawaguchi¹, Daiki Towa¹, Yong-Chang Lau^{1,2}, Saburo Takahashi² and Masamitsu Hayashi^{1,2*}

¹*Department of Physics, The University of Tokyo, Bunkyo, Tokyo 113-0033, Japan*

²*National Institute for Materials Science, Tsukuba 305-0047, Japan*

³*Institute for Materials Research, Tohoku University, Sendai 980-8577, Japan*

S1. Extraction of the thickness dependent resistivity

The sheet conductance G_{XX} is evaluated for each sample in order to calculate distribution of the current within the bilayer. We use four-point probe technique to measure the resistance R_0 (see the main text for the definition of R_0) of a Hall bar (width: w , distance between the voltage probes: L). The sheet conductance is defined as $G_{XX}=L/(wR_0)$. Figure S1 shows the sheet conductance of the Pt/Co bilayers as a function of Pt (d_N) and Co (t_F) thicknesses. Clearly G_{XX} depends on t_F and d_N . We use second degree polynomial fitting to extract the thickness dependent intrinsic resistivity. Note that the Fuchs-Sondheimer model gives such dependence when the layer thickness is smaller than its mean free path. The solid lines in Fig. S1 shows the fitted curves $f(d_N, t_F)$ using a parabolic function. To determine the conductivity of each layer as a function of d_N or t_F , we take the thickness derivative of $f(d_N, t_F)$ and define the conductivities as follows:

$$\sigma_N(t_F, d_N) \equiv \frac{\partial f(t_F, d_N)}{\partial d_N} \quad (\text{S1})$$

$$\sigma_F(t_F, d_N) \equiv \frac{\partial f(t_F, d_N)}{\partial t_F} \quad (\text{S2})$$

Here, σ_N and σ_F are the conductivity of Pt and Co, respectively. The resistivity is obtained using the following relations: $\rho_{\text{Pt}} \sim 1/\sigma_N$ and $\rho_{\text{Co}} \sim 1/\sigma_F$ (here we have neglected the transverse component of the conductivity). ρ_{Pt} and ρ_{Co} are displayed in Figs. 1(b) and 1(c), respectively.

S2. W/Co and W/CoFeB bilayers

To check whether the combination of Pt and Co is essential to observing the unusually large SMR, we have studied the FM layer thickness dependence of HM/FM bilayers with HM=W and FM=Co and CoFeB. The films are made by RF magnetron sputtering. The film structure is sub. | 3 W | t_F Co | 2 MgO | 1 Ta and sub. | 3 W | t_F CoFeB | 2 MgO | 1 Ta (units of the thickness is nm). Films are annealed at 300 °C for 1 hour ex-situ in vacuum. Results from these films are presented in Fig. S2.

S3. Anomalous Hall resistance

The Pt layer thickness dependence of the anomalous Hall resistance R_{AHE} is shown in Fig. S3. R_{AHE} is the difference in the Hall resistance R_{XY} when the magnetization of the Co layer points along $+z$ and $-z$. R_{AHE} is divided by the sheet resistance R_{XX} and $(1-x_N)$: the anomalous Hall angle

θ_{AH} of the FM layer corresponds to $-R_{AHE}/R_{XX}/(1-x_N)$ if one neglects contribution of the diffusive spin current from the Pt layer on the Hall resistance¹.

S4. Model calculations

The Pt and Co layer thickness dependence of R_{SMR} calculated using Eq. (2) of the main text is shown in Fig. S4, black solid lines. The following parameters are used in the calculations. Co layer: $\theta_F=0.075$, $\theta_{AH}=0.03$, $P=0.4^2$, $\lambda_F=40$ nm (ref. ²). Pt layer: $\theta_{SH}=0.2$ (ref. ³), $\lambda_N=1$ nm. The resistivity of each layer is taken from Fig. 1. Interface: $\text{Re}[G_{MIX}]=10^{14} \Omega^{-1}\text{cm}^{-2}$, $\text{Im}[G_{MIX}]=10^{10} \Omega^{-1}\text{cm}^{-2}$. Note that such G_{MIX} represents a transparent Pt/Co interface for spin transmission. To illustrate the effect of spin transport in the Co layer on the SMR, the blue solid lines in Fig. S4 show R_{SMR} calculated with the same parameters as above but with $\theta_F=0$ and $\theta_{AH}=0$.

S5. Influence of IMR on SMR

In order to evaluate how IMR influences the SMR, we subtract IMR from ΔR_{y-z} and extract SMR with the assumption that IMR in the $y-z$ plane has the same magnitude with that of $x-z$ plane. To model the system, we assume that the resistance change due to SMR occurs in the HM layer (e.g. Pt) whereas the change caused by the IMR takes place within the FM layer (e.g. Co). One can therefore consider a parallel circuit that describes the magnetoresistance due to SMR and IMR as the following. We define the change in the current when the magnetic field is applied along the y -axis and z -axis as ΔI . As noted above, ΔI can be divided into two components, changes that occur in the FM layer (ΔI_{FM}) and the HM layer (ΔI_{HM}).

From the parallel circuit model, we obtain

$$\Delta I = \Delta I_{HM} + \Delta I_{FM} \quad (\text{S3})$$

ΔI can be expressed using the average film resistivity ρ and its change $\Delta\rho$ due to the field application along y and z , film thickness $t=d_N+t_F$ and the voltage V applied across the films as:

$$\Delta I = Vt\left(\frac{1}{\rho+\Delta\rho} - \frac{1}{\rho}\right) \quad (\text{S4})$$

Similarly, using the parameters defined in the main text, we obtain

$$\Delta I_{HM} = Vd_N\left(\frac{1}{\rho_N+\Delta\rho_N} - \frac{1}{\rho_N}\right) \quad (\text{S5})$$

$$\Delta I_{FM} = Vt_F\left(\frac{1}{\rho_F+\Delta\rho_F} - \frac{1}{\rho_F}\right) \quad (\text{S6})$$

Note that here we assume contribution from the transverse resistivity on the longitudinal current is negligible. We define the resistivity change ratio in the HM and the FM layer as $R_{SMR} = \Delta\rho_N/\rho_N$ and $R_{IMR} + \Delta R_{y-z}^{Co} = \Delta\rho_F/\rho_F$, respectively, and the average ratio within the film as $\Delta R_{y-z} = \Delta\rho/\rho$. Equations (S3)-(S6) can be put together to read:

$$\frac{\Delta R_{y-z}}{(1+\Delta R_{y-z})} \left(\frac{t_F}{\rho_F} + \frac{d_N}{\rho_N}\right) = \frac{R_{SMR}}{(1+R_{SMR})} \frac{d_N}{\rho_N} + \frac{R_{IMR}+\Delta R_{y-z}^{Co}}{(1+R_{IMR}+\Delta R_{y-z}^{Co})} \frac{t_F}{\rho_F} \quad (\text{S7})$$

Assuming $\Delta R_{y-z}, R_{SMR}, R_{IMR} \ll 1$, we obtain

$$\Delta R_{y-z} \left(\frac{t_F}{\rho_F} + \frac{d_N}{\rho_N}\right) = (R_{IMR} + \Delta R_{y-z}^{Co}) \frac{t_F}{\rho_F} + R_{SMR} \frac{d_N}{\rho_N} \quad (\text{S8})$$

Rearranging Eq. (S8) will give the relation described in the main text.

References

- 1 Peng Sheng, Yuya Sakuraba, Yong-Chang Lau, Saburo Takahashi, Seiji Mitani, and Masamitsu Hayashi, "The spin Nernst effect in tungsten." *Science Advances* **3**, e1701503 (2017).
- 2 J. Bass and W. P. Pratt, "Current-perpendicular (CPP) magnetoresistance in magnetic metallic multilayers." *J. Magn. Magn. Mater.* **200**, 274 (1999).
- 3 Weifeng Zhang, Wei Han, Xin Jiang, See-Hun Yang, and Stuart S. P. Parkin, "Role of transparency of platinum-ferromagnet interfaces in determining the intrinsic magnitude of the spin Hall effect." *Nat. Phys.* **11**, 496 (2015).

Figure captions

Figure S1. (a) Pt layer thickness dependence of the sheet conductance G_{XX} and (b) Co layer thickness dependence of G_{XX} in Pt/Co bilayers. Lines are fit to the data using a parabolic function.

Figure S2. (a,b) Ferromagnetic metal (FM) layer thickness dependence of the sheet conductance (G_{XX}) of HM/FM bilayers. The heavy metal (HM) layer is W. FM=Co (a) and FM=CoFeB (b). The solid lines show fit to the data in selected FM thickness ranges. Resistivity (ρ_F) extracted from the fitting are displayed in each panel. (c,d) ΔR_{y-z} (solid squares) and $\Delta R_{y-z}/x_N$ (open circles) vs. FM layer thickness for W/FM bilayers. FM=Co (c) and FM=CoFeB (d). Lines are guide to the eyes.

Figure S3. (a-e) Pt (d_{Pt}) layer thickness dependence of the anomalous Hall resistance R_{AHE} divided by the sheet resistance R_{XX} and $(1-x_N)$. The thickness of the Co layer is indicated in each panel.

Figure S4. (a-e) Calculated spin Hall magnetoresistance (R_{SMR}) plotted as a function of the Pt layer thickness (d_{Pt}) for fixed Co layer thicknesses. (f-j) Calculated R_{SMR} vs. Co layer thickness (t_{Co}) for fixed Pt layer thicknesses. The thickness of the fixed thickness layer is noted in each panel. Parameters used in the calculations are described in the text. The black solid lines show R_{SMR} calculated using Eq. (2) with the parameters described in the text. The blue solid lines are calculated similarly except for θ_F and θ_{AH} , which are both set to 0.

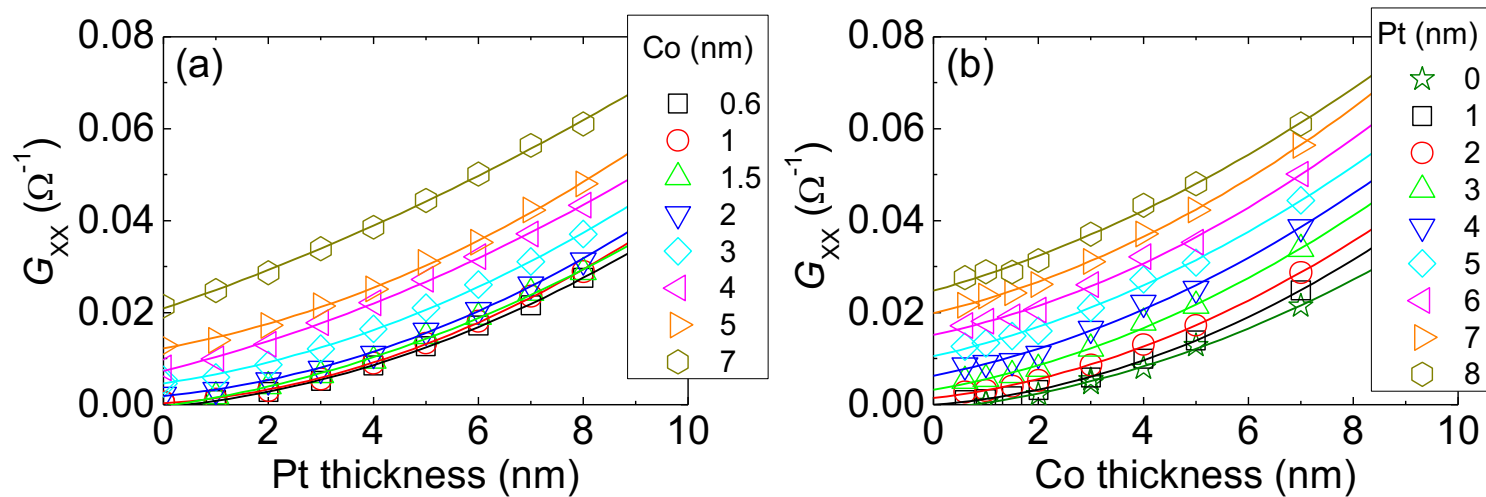


Fig. S1

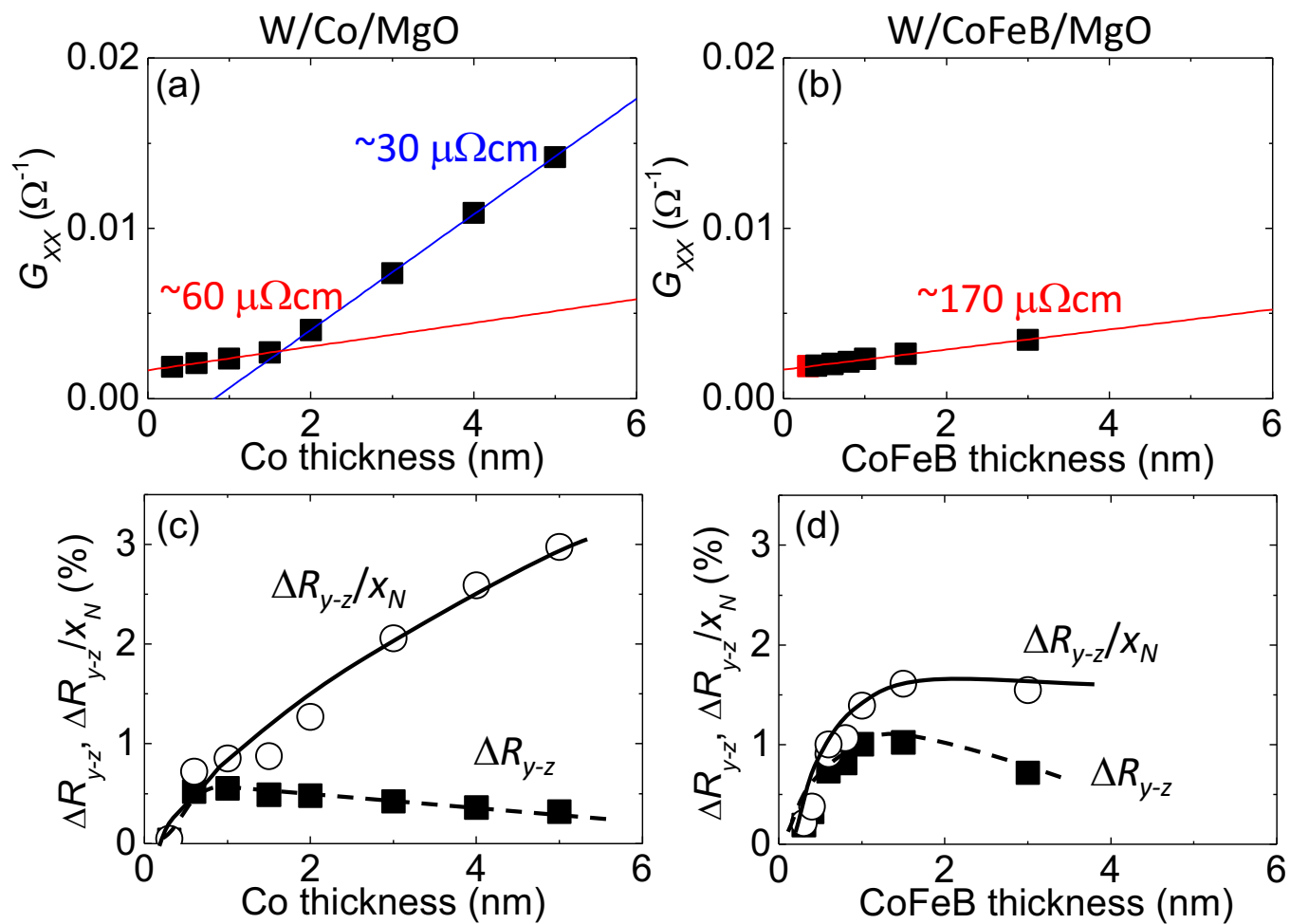


Fig. S2

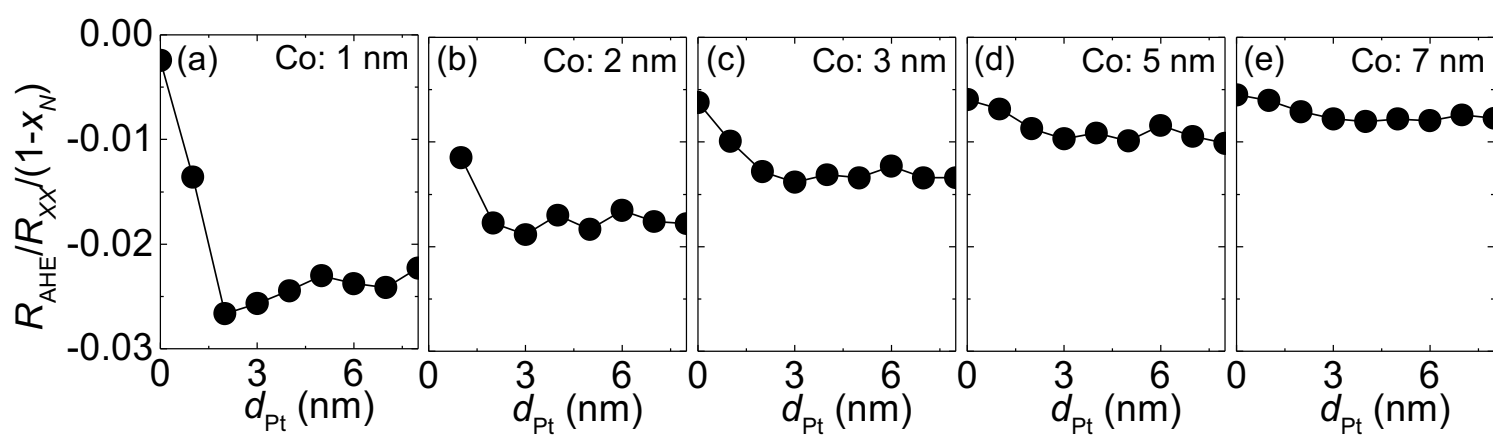


Fig. S3

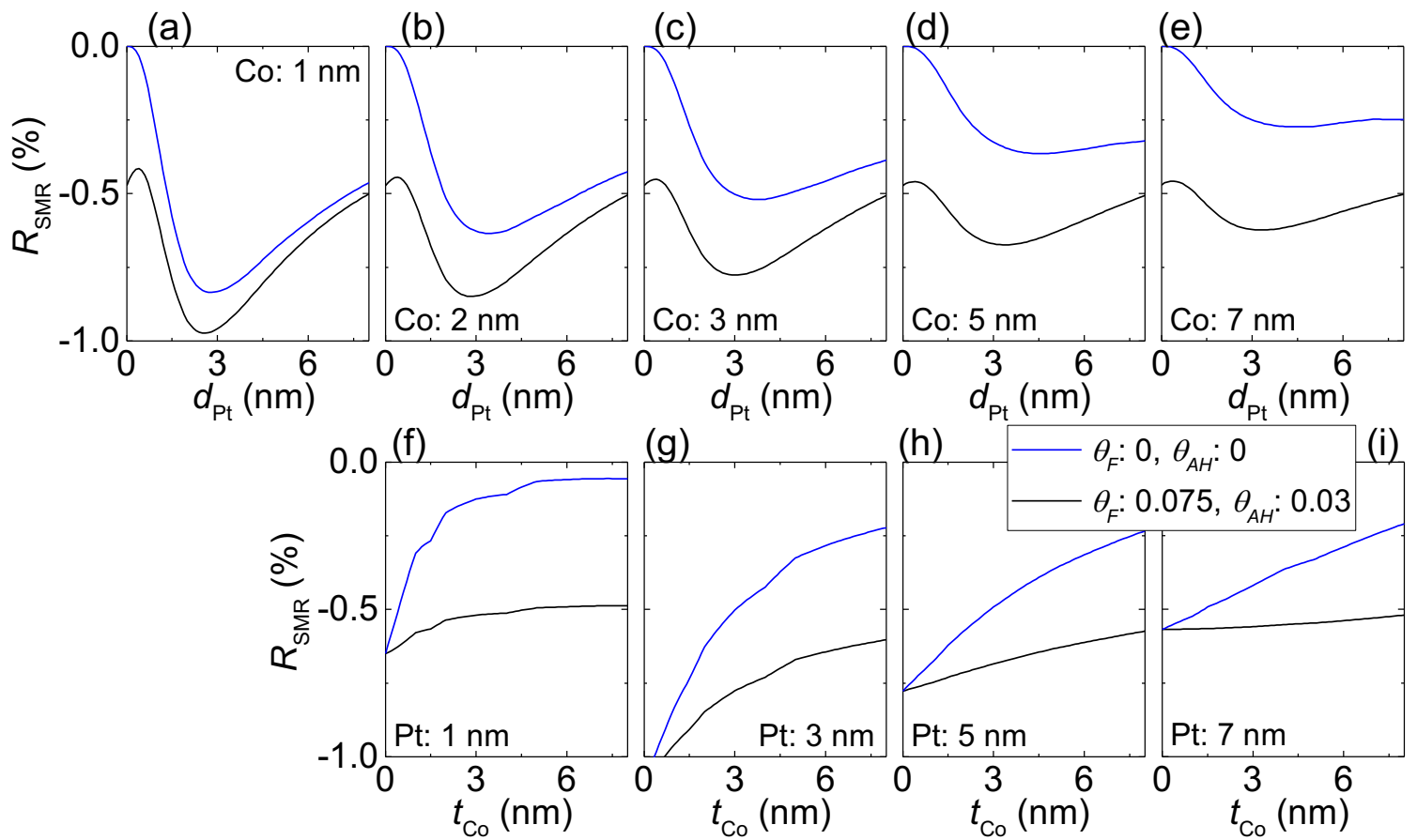


Fig. S4